Available online www.worldscientificnews.com

World Scientific News

An International Scientific Journal

WSN 214 (2026) 198-221

EISSN 2392-2192

Analytical Modeling for Transport (Nano-)Processes

Paolo Di Sia[1-4]

[1]School of Engineering & School of Medicine, University of Padova, 35131 Padova, Italy
E-mail address: paolo.disia@unipd.it
[2]Engineering for Innovation Medicine, University of Verona, 37134 Verona, Italy
E-mail address: paolo.disia@univr.it
[3]"Primordial Dynamic Space" Research, 37134 Verona, Italy
E-mail address: paolo.disia@gmail.com
[4]ORCID: 0000-0002-6405-0483

https://doi.org/10.65770/KFFB9968

ABSTRACT

Nano-bio-technologies are a new interdisciplinary scientific sector, with revolutionary perspectives due to the fact that, at nano-size, the behavior and characteristics of matter radically change with respect to macroscopic dimensions. The paper provides an overview of the mathematical analytical modeling for transport (nano-)processes, through which the phenomena of charge transport (at nanometer level) are considered (also with reference to the most used numerical methods); it considers also recent advances in analytical (nano-)modeling. Plasmonics and related applications are also described. Examples of application are collected in the Appendix.

***Keywords*:** Theoretical (Analytical) Modeling, Drude-Lorentz-type Models, DS Model; Transport Processes, Nano-Physics, Nano-Bio-Technology, Plasmonics.

(Received 20 February 2026; Accepted 18 March 2026; Date of Publication 17 April 2026)

1. INTRODUCTION

One of the most important aspects at nanoscale is the charge transport, which can be influenced by particles dimensions and demonstrates different characteristics with respect to those of bulk. If the mean free path of charges is larger than the particle dimensions, we have a mesoscopic system in which the transport depends by dimensions. A similar situation occurs also in thin films, where the smallest nanostructure dimension can be less than the free displacement, then requiring variations to existing transport bulk models.

A rigorous knowledge of transport properties is therefore to be considered as a priority. From a theoretical point of view, several techniques have been used for the comprehension of transport phenomena, and particularly powerful are the analytical descriptions, of high mathematical interest, high elegance, and suitable to be implemented through experimental data from literature.

To set the applicability limit of a bulk model and to inquire the time response of systems, in particular at the nanoscale, one of the crucial experimental technique for the study of the frequency-dependent complex-valued far-infrared photo-conductivity $\sigma(\omega)$ is the Time-resolved THz Spectroscopy (TRTS).

It is an ultrafast non-contact optical probe; experimental data are usually fitted through "Drude-Lorentz", "Drude-Smith" or "Effective Medium" models. A particular strength is showing to have a recent theoretical analytical approach, based on the correlation function obtained by a complete Fourier transform of $\sigma(\omega)$, said DS model [1]. Thanks to it, we can use the analytical expressions of the most important transport functions:

a) the velocities correlation function $\langle \vec{v}(t)\cdot\vec{v}(0)\rangle_T$ at the temperature T;

b) the mean square deviation of position $R^2(t)=\left\langle [\vec{R}(t)-\vec{R}(0)]^2 \right\rangle$;

c) the diffusion coefficient $D(t)=\frac{1}{2}\left(dR^2(t)/dt\right)$.

In the following, we illustrate an overview of the fundamental models that, historically starting by the Drude model, analyze the transport phenomena of matter, in particular at the nanoscale, coming to the last developments, which involve, inter alia, the concept of plasmon.

The "Finite Element Method" (FEM) is often used; it allows the decomposition of a complex/articulated problem into a set of several simpler problems through the process of discretization. After solving them and reassembling the individual solutions, we reconstruct the initial one [2-4].

At mesoscopic scale, experimental results, not explainable with the classical mechanics of materials, meet an effective explanation with nano-mechanics [5,6]. A single model is often not satisfactory to completely describe the behavior of the medium at the nanoscale, leading to the concept of "multiscale modeling" [7,8].

Several techniques have been used for the knowledge of transport phenomena, divided between analytical descriptions grounded on transport equations and numerical approaches, as classical and quantum Monte Carlo simulations [9].

An important group of models is that of the “Drude-Lorentz-type” models, variations, and extensions of the Drude-Lorentz and Smith models. Fully analytical models, besides being mathematically very attractive, are rigorous and less time-consuming than the others.

The next paragraphs deal with the “Semi-empirical and Ab initio” formulations (§ 2), the “Molecular Dynamics” (MD) simulation (§ 3), the “Atomic-scale Finite Element” method (AFEM) (§ 4), “Multi-scale” computational methods (§ 5), Basics of “Plasmonics” (§ 6), the best known “Drude-Lorentz-type” models (§ 7), the “quantum-relativistic DS” model (§ 8) and the concluding remarks (§ 9). Appendix (§ 10) summarizes various examples of application.

2. “SEMI-EMPIRICAL AND AB INITIO” FORMULATIONS

The most used semi-empirical formulations are as follows:

I) the “Tight-Binding” Method (T-BM): it is a semi-empirical method, often preferred when the computational calculation is consistent, taking care in the choice of used parameters. It is based on the method of linear combination of atomic orbitals (LCAO), proposed by Bloch in 1928 and then revised by Slater and Koster in 1954 [10].

It utilizes the Schrödinger equation:

$$H|\Psi\rangle = E|\Psi\rangle \tag{1}$$

where $|\Psi\rangle$ is the wave function of the electron in the Dirac notation. Its resolution is equivalent to the minimization of the energy functional:

$$E = \frac{\langle\Psi|H|\Psi\rangle}{\langle\Psi|\Psi\rangle} \tag{2}$$

with $\langle\Psi|\Psi\rangle = 1$.

The minimization brings to:

$$\delta\left(\langle\Psi|\vec{H} - E\vec{I}|\Psi\rangle\right) = 0. \tag{3}$$

II) The “Ab-initio” formulations allow accurate results, although dependent by peculiar choices, as that of the basis functions.

II$_1$) “Density Functional” Theory (DFT): it formulates the total energy of the system by means of the functional of the electrons total density [11]. The energy of a system constituted by a determined number of electrons is writable as:

$$E = T\left[\rho(\vec{r})\right] + V\left[\rho(\vec{r})\right] + E_{exch}\left[\rho(\vec{r})\right] \tag{4}$$

(T, V = kinetic energy of electrons and potential energy of electrons-nuclei and nucleus-nucleus, respectively).

E_{exch} is the exchange functional, depending by the adopted approach. The outer electrons (valence electrons) are considered; inner electrons and nuclei are treated together as ions.

ii2) "Local Density Functional" Theory (LDFT): the exchange functional is written as:

$$E_{exch}=\int\rho(\vec{r})\varepsilon_{exch}(\rho(\vec{r}))d\vec{r} \tag{5}$$

with ε_{exch} exchange energy of the electron inside an electron cloud with constant density [12]. For a system of N electrons, the electrons density function follows the Kohn-Sham form for the orbital of a single electron Ψ_i:

$$\rho(\vec{r})=\sum_{i=1}^{N}\left|\Psi_i(\vec{r})\right|^2=\sum_{i=1}^{N}\Psi_i^*(\vec{r})\Psi_i(\vec{r}). \tag{6}$$

LDFT is a rather rough approximation of the molecular system, assuming a uniform electrons density in the molecular system.

About further approaches, we remember:

III1) the "Non-Local Functional Approach" (N-LFA): the energy of the system depends by a density gradient of the electrons too [13];

III2) the "Car-Parrinello Molecular Dynamic Method" (C-PMDM): it usually employs periodic boundary conditions, plane wave basis sets, density functional theory [14];

III3) the "Conjugate-Gradient Method" (C-GM): it is an iterative method for the numerical solution of particular systems of linear equations, applied to sparse systems, too large to be handled by direct methods [15];

III4) the "Augmented Plane Wave Method" (APWM): it is used for approximating the energy states of electrons in a crystal lattice; the potential is assumed as spherically symmetric within spheres centered at each atomic nucleus and constant in the interstitial region [16];

III5) the "Korringa-Kohn-Rostoker Method" (K-K-RM): it is a Green's function method, used for calculating the electronic band structure of solids [17];

III6) the "Linearized-Muffin-Thin-Orbital Method" (L-M-T-OM): it is a specific implementation of the density functional theory within the local density approximation (LDA) [18];

III7) the "Full Potential Linearized Augmented Plane Wave Method" (FPLAPWM): used as ab initio electronic structure technique with reasonable computational efficiency [19].

3. "MOLECULAR DYNAMICS" (MD) SIMULATION

The simulations of the behavior at atomic level are used for situations in which the model dimensions are too large for a quantum simulation, but an atomic scale of the problem is needed [20].

They are based on two basic assumptions:

a) the molecules or atoms are described as a system of interacting material points, and the motion is dynamically described by position vectors and instantaneous velocities;

b) there is no mass changes, and the system is treated as an isolated domain.

The equations of motion for a system of interacting material points (particles or atoms), with f degrees of freedom, can be written in terms of a Lagrangian of the form:

$$\frac{d}{dt}\frac{\partial L}{\partial \dot{q}_f}-\frac{\partial L}{\partial q_f}=0 \tag{7}$$

with $f = 1, 2, 3, \ldots, k$.

The MD simulation pertains to a Cartesian coordinate system, where Eq. (7) becomes:

$$\frac{d}{dt}\frac{\partial L}{\partial \dot{r}_i}-\frac{\partial L}{\partial r_i}=0 \tag{8}$$

with $i = 1, 2, 3, \ldots, N$.

A possible function for non-interacting particles in $\Re^3$ is as follows:

$$L=\sum\nolimits_{i=1}^{N}\frac{m_i\,\dot{r}_i^2}{2}=\sum\nolimits_{i=1}^{N}\frac{m_i}{2}\left(\dot{x}_i^2+\dot{y}_i^2+\dot{z}_i^2\right) \tag{9}$$

Considering the particles interaction, Eq. (9) becomes:

$$L=\sum\nolimits_{i=1}^{N}\frac{m_i\,\dot{r}_i^2}{2}-U\left(r_1, r_2, \ldots, r_N\right) \tag{10}$$

where U is the potential. In Newtonian form, we have:

$$F_i=m_i\frac{d^2 r_i}{dt^2}=-\frac{\partial U\left(r_i\right)}{\partial r_i} \tag{11}$$

with F_i inner force on the i-th atom.

An alternative to the Lagrangian function in terms of generalized coordinates and momentum is the formulation of Hamilton:

$$d\left(p_f\,d\dot{q}_f-L\right)=-\frac{\partial L}{\partial q_f}dq_f+\dot{q}_f\,dp_f-\frac{\partial L}{\partial t}dt \tag{12}$$

The Hamiltonian function is:

$$d\,H=-\frac{\partial L}{\partial q_f}dq_f+\dot{q}_f\,dp_f-\frac{\partial L}{\partial t}dt \tag{13}$$

with:

$$H(p,q,t)=\sum\nolimits_i \dot{q}_f\,p_f-L(p,q,t) \tag{14}$$

and it is:

$$\dot{p}_f = -\frac{\partial H}{\partial q_f}; \quad \dot{q}_f = \frac{\partial H}{\partial p_f}; \quad \frac{\partial H}{\partial t} = -\frac{\partial L}{\partial t} \tag{15}$$

For a conservative system of M interacting atoms in a Cartesian system, the Hamiltonian function can be re-written as $H(r_1, r_2, \ldots.., r_M, p_1, p_2, \ldots.., p_M)$, with $\dot{r}_i = \frac{\partial H}{\partial p_i}; \; \dot{p}_i = -\frac{\partial H}{\partial r_i}$.

Knowing the Hamiltonian function and the initial state of the system atoms, we can calculate positions and momentum in following instants.

About the representation of the inter-atomic interaction of a system, two important potentials classes can be considered:

a) "Pair" potentials, between pairs of atoms;
b) "Multi-Body" potentials.

About a), we underline:

a_1) "Hard/Soft" spheres: this is the simplest potential, useful for theoretical investigations of some ideal problems. The form is:

$$(Hard) \quad U(r_{ij}) = \begin{array}{l} \infty \;\; for \;\; r_{ij} \le r_0 \\ 0 \;\; for \;\; r_{ij} > r_0 \end{array} \tag{16}$$

$$(Soft) \quad U(r_{ij}) = \left(\frac{r_{ij}}{r_0}\right)^{-n} \tag{17}$$

with: $|r_{ij}| = |r_i - r_j|$ [21].

a_2) The "Lennard-Jones" potential, for describing the interaction between pairs of atoms:

$$U(r_{ij}) = 4E_b\left(\left(\frac{D}{|r_i - r_j|}\right)^{12} - \left(\frac{D}{|r_i - r_j|}\right)^{6}\right) \tag{18}$$

(E_b = binding energy; D = diameter of collision).

The first term represents the atomic repulsion, the second one the attraction. It describes the interaction of van der Waals forces in molecular systems and inert gases (Ar, Kr, CH_4, O_2, H_2, C_2H_4, etc.) [22].

a_3) The "Morse" potential:

$$U(r_{ij}) = E_d\left(e^{2a(L_{eq}-r)} - 2e^{a(L_{eq}-r)}\right) \tag{19}$$

(L_{eq} = equilibrium length, E_d = dislocation energy, a = scale factor as inverse of length).

b) Multi-Body potentials are used to explain phenomena of “stiction“ and “snap-back”, as well as for the analysis of the molecular mechanisms under large deformation and for the resistance to fracture [23].

4. “ATOMIC-SCALE FINITE ELEMENT” METHOD (AFEM)

The equilibrium configuration of a M atoms system corresponds to the state of minimum total energy. Denoting with $E_{tot}(x)=E_{tot}(x_1, x_2, ..., x_M)$ the function which defines the total system energy, the state of equilibrium is identified by:

$$\frac{\partial E_{tot}(x)}{\partial x}=0. \tag{20}$$

In the context of “Molecular Dynamics” (MD) simulation, an inter-atomic potential is considered as a tool for determining the forces acting among atoms. For finding the equilibrium configuration, potentials with values depending on the material parameters and the mutual position of atoms are used. The equation governing the problem is the same that governs the continuous FEM modeling: $K v=P$.

AFEM is specific for changeable materials, while FEM modeling is generic for all materials, because an AFEM element depends by the inter-atomic potentials, which is different for each material [24].

5. “MULTI-SCALE” COMPUTATIONAL METHODS

Multi-scale computational methods have been designed for the study of materials and systems at different scales of investigation. Among the fields in which the modeling has given interesting results, we remember the fracture mechanics, comprising the crack propagation and the dislocation emission. In the representation of crystalline materials, it is used a Lennard-Jones potential to describe the interaction of the grains at mesoscopic scale [25-27].

6. BASICS OF “PLASMONICS”

One of the most interesting phenomena in nano-structures are electromagnetic resonances, due to collective oscillations of the conduction electrons, said “plasmons”. They are excited by light, leading to light scattering, absorption, and to an increase of the local electromagnetic field. The interest for plasmons intersects the growing demand of technology, particularly for semiconductor based integrated electronic components, optical applications, new nano-components, and development processes, as the guide of light in integrated optical systems and the interface with electronic components [28].

The concept of plasma is decidedly useful in the description of some aspects of the interaction radiation/conductive matter; the free electrons of the conductive material (for example, a metal) are considered as an electron fluid with high density, of order of $10^{23}\, cm^{-3}$.

This concept is the starting point of the classic Drude model (stopped positive ions and a gas of classical not interacting electrons), with motion slowed by a force of viscous friction characterized from a relaxation time τ. The plasma frequency is defined as the proper frequency of the collective motion of electrons in the following way:

$$\omega_p^2 = \frac{\sigma_0}{\varepsilon_0 \tau} = \frac{n e^2}{\varepsilon_0 m} \tag{21}$$

with σ_0 conductivity of material. The dielectric constant of metal can be written as a function of ω_p:

$$\varepsilon(\omega) = 1 - \frac{\omega_p^2}{\omega^2} \tag{22}$$

From the comparison between ω and ω_p, we can deduce the behavior of the electromagnetic waves arriving to the metal. The plasma oscillations are the fluctuations of charge density, which happen to the frequency ω_p and propagate in the metal. The quanta of such fluctuations inside the volume are the “volume plasmons”; the mechanism on the metal surface is characterized by the “(localized) surface plasmons” [29].

Modeling concerning plasmonics simulates the extinction of the “localized surface plasmons resonance” (LSPR) from nanoparticles and nanoarrays, with the calculation of the light absorption and the scattering. The most used models are:

I) the “Mie” theory [30];
II) the “Gans” theory [31];
III) the “discrete-dipole approximation” method (DDA) [32];
IV) the “finite-difference time-domain” method (FDTD) [33].

I) The Mie theory concerns the optical properties of nanoparticles. When their dimension is smaller than the wavelength of the incident light, the extinction caused from a metallic nanosphere is estimated in the quasi-static and dipole limit. The relative cross section of the process results in:

$$\sigma_{ext} = \frac{24 \pi N_A a^3 \varepsilon_m^{3/2}}{\lambda \ln(10)} \left[\frac{\varepsilon_i}{(\varepsilon_r + \chi \varepsilon_m)^2 + \varepsilon_i^2} \right] \tag{23}$$

(N_A = surface density; a = radius of the metallic nanosphere; ε_m = dielectric constant of the medium surrounding the nanosphere; λ = wavelength; $\varepsilon_i, \varepsilon_r$ = imaginary and real part of the dielectric function of the metallic nanosphere respectively; χ = form factor concerning the nanoparticle).

II) The Gans theory extends the Mie theory to the case of spheroidal particles. About the cross section of the process, we can write (case of polarization of incident light parallel to the symmetry axis of the spheroid):

$$\sigma_{ext} = \frac{2\pi V \varepsilon_m^{3/2}}{3\lambda} \sum_j \left[\frac{(1/P_j)^2 \varepsilon_j}{(\varepsilon_r + \frac{1-P_j}{P_j}\varepsilon_m)^2 + \varepsilon_j^2} \right] \tag{24}$$

(V = volume of nanoparticle, P_j = depolarization factors, holding into account of the anisotropic form of particles).

III) With the DDA method, nanoparticles are divided in a cubic array of N polarizable dipoles, with polarizabilities α_i determined by the dielectric function of nanoparticles. The induced dipole P_i of every element is $P_i = \alpha_i E_{loc,i}$; the cross section is given by:

$$\sigma_{ext} = \frac{4\pi k}{\left|\vec{E}_{inc}\right|^2} \sum_{j=1}^{N} \mathrm{Im}\left(\vec{E}_{inc,j}^{\;*} \cdot \vec{P}_j\right) \tag{25}$$

with $k = \omega/c$ (in vacuum). The applications range the calculation of the absorption, scattering, extinction, and other optical properties of nanoparticles of different forms and dimensions.

IV) The FDTD method (FDTD) resolves the Maxwell equations in the time domain, covering a wide frequency range with a single process of simulation, useful in applications where the resonance frequencies are not exactly known.

7. “DRUDE-LORENTZ-TYPE” MODELS

Historically, the two main models of the elementary theory of metals have been:

1) The “Drude” model, based on the kinetic theory of an electron gas in a solid. It assumes that all electrons have the same average kinetic energy E_m ;

2) The “Sommerfeld” model, variation of the previous one, integrated with the foundations of quantum mechanics.

In the Drude model, all electrons move as an electronic gas, and the ideal gas equations are applied, even if the electron gas is dense. Free electrons have kinetic energy and no potential energy, implying the possibility to apply the kinetic theory of gases to such electronic gas. The relaxation time τ is defined as the average time between two collisions. The current density is $\vec{J} = \sigma_{cond} \vec{E}$ (σ_{cond} = electric conductivity) [34,35].

3) The “Drude-Lorentz” model: this is an improving of the Drude model, in which the statistical aspects are specified. Electrons are considered as free charges, described by a Maxwellian velocity distribution. If we consider an electron gas in a spatial region with a constant electric field, the drift velocity of electrons is constant, corresponding to a current density $\vec{J}$ proportional to the applied field $\vec{J}=\sigma_0 \vec{E}$, with $\sigma_0 = ne^2 \tau / m$ (n = electron density). The presence of an electric field of the form $E(t)=E_0 e^{-i\omega t}$ brings to a complex conductibility of the form $\sigma_\omega = \sigma_0 /(1-i\omega\tau)$.

4) “Drude-Lorentz-like” models:

4a) the “Maxwell-Garnett” model (MG): it describes an isotropic matrix containing isolated spherical inclusions, like metal particles dispersed in a surrounding host matrix. The dielectric function is given by a Drude term with an additional “vibrational” contribution at a finite frequency ω_o:

$$\varepsilon_{//}(\omega)=1-\frac{\omega_p^2}{\omega(\omega+i/\tau)}+\frac{\omega_s^2}{\omega_0^2-\omega^2-i\gamma\omega} \tag{26}$$

(amplitude ω_s, resonant frequency ω_0, and damping constant γ depend by the particular considered material).

4b) the “Bruggeman” model (BR): it is mainly used for the study of the effective conductivity of systems composed of multi-component spherical inclusions with different conductivity. In the case of circular and spherical inclusions, we have:

$$\sum_i \delta_i \frac{\sigma_i-\sigma_e}{\sigma_i+(n-1)\sigma_e}=0 \tag{27}$$

(n = spatial dimension; δ_i (with $\sum_i \delta_i = 0$) and σ_i = fraction and conductivity of each component respectively; σ_e = effective conductivity of the medium). The sum is performed on all constituents. For elliptical and ellipsoidal inclusions, Eq. (27) becomes:

$$\frac{1}{n}\delta\alpha+\frac{(1-\delta)(\sigma_m-\sigma_e)}{\sigma_m+(n-1)\sigma_e}=0 \tag{28}$$

which generalizes Eq. (27) for a two-phase system with conductivity inclusions σ_e in a matrix of conductivity σ_m. For randomly oriented inclusions, α is given by:

$$\alpha=\sum_{j=1}^{n}\frac{\sigma-\sigma_e}{\sigma_e+L_j(\sigma-\sigma_e)} \tag{29}$$

(L_j (with $\sum_j L_j = 0$) = appropriate doublets/triplets depolarization factors, governed by the ratio between the axes of the ellipse or ellipsoid).

4c) “Effective medium” theories (EMTs): in this case, the electromagnetic interactions among pure materials and host matrices are roughly taken into account. They include the Maxwell-Garnett model and the Bruggeman model. In the THz regime, the dielectric function $\varepsilon_m(\omega)$ usually includes contributions of the high-frequency dielectric constant, free electrons of conduction and lattice vibration [36]. The form of the dielectric function is:

$$\varepsilon_m(\omega)=\varepsilon_\infty-\frac{\omega_p{}^2}{\omega^2+i\gamma\omega}+\sum_j\frac{\varepsilon_{st_j}\,\omega_{TO_j}{}^2}{\omega_{TO_j}{}^2-\omega^2-i\Gamma_j\,\omega} \tag{30}$$

(ε_∞ = high-frequency dielectric constant, the second term is related to the contribution of free electrons or plasmons, the last term considers the optical phonons).

In the case of main contribution of free electrons or plasmons, Eq. (30) is replaced by:

$$\varepsilon_m(\omega)=\varepsilon_\infty-\frac{\omega_p{}^2}{\omega^2+i\gamma\omega} \tag{31}$$

Eq. (31) proficiently describes the dielectric properties of metals and semiconductors.

In the case of a dominant role of a radiation field with the fundamental lattice vibration, resulting in absorption of electromagnetic wave, the $\varepsilon_m(\omega)$ expression is:

$$\varepsilon_m(\omega)=\varepsilon_\infty+\frac{\varepsilon_{st}\,\omega_{TO}{}^2}{\omega_{TO}{}^2-\omega^2-i\gamma\omega} \tag{32}$$

5) The Smith model: it starts by the response theory for the optical conductivity, examining the response in resulting current $j(t)$, and using for the complex frequency-dependent conductivity the Fourier transform:

$$\tilde{\sigma}(\omega)=\int_0^\infty j(t)\exp(i\omega t)\,dt \tag{33}$$

with:

$$j(0)=n^*e^2/m \tag{34}$$

(n^* = effective electron density). It holds:

$$\int_0^\infty \mathrm{Re}\,\tilde{\sigma}(\omega)\,d\omega=\frac{\pi}{2}j(0)=\frac{\omega_p^2}{8} \tag{35}$$

with $\omega_p=\sqrt{n^*e^2/(\varepsilon_0 m)}$ plasma frequency. If the initial current decays exponentially to its initial value with relaxation time τ, we get the standard Drude formula:

$$\tilde{\sigma}(\omega)=(n^{*}e^{2}\,\tau/m)/(1-i\,\omega\tau) \tag{36}$$

which can be considered as the first term of the series:

$$j(t)/j(0)=\exp(-t/\tau)\left[1+\sum_{n=1}^{\infty}c_{n}\left(t/\tau\right)^{n}/n!\right] \tag{37}$$

The c_n factors consider the original electrons speed remained after the *n*-th collision and allow the generalization of the Drude formula [4,37]. The analytical form of the complex conductivity is:

$$\tilde{\sigma}(\omega)=\frac{n^{*}e^{2}\,\tau}{m(1-i\,\omega\tau)}\left[1+\sum_{n=1}^{\infty}\frac{c_{n}}{(1-i\,\omega\tau)^{n}}\right] \tag{38}$$

8. “QUANTUM-RELATIVISTIC DS” MODEL

The “DS” model is a recent generalization of the Drude-Lorentz model with the great merit of being completely analytical, thus avoiding the numerical approach, which is approximate and more time consuming [1]. It considers the transition between classical and quantum regime occurring at the nanometer length scale, in agreement with the comparability of the de Broglie wavelength of thermal electrons and the length of the system.

This model generalizes the classical Drude-Lorentz formula based on linear response theory and of the resonant plasmonic mode, adding to the classic treatment the description at quantum and relativistic level.

One of the new ideas of the DS model is the use of the following relation:

$$<\vec{v}^{\alpha}(0)\,\vec{v}^{\beta}(t)>_{T}=\frac{KTV}{\pi e^{2}}\int_{-\infty}^{+\infty}d\omega\,\mathrm{Re}\,\sigma_{\beta\alpha}(\omega)\,e^{i\omega t} \tag{39}$$

i.e. the possibility to perform a complete inversion on temporal scale, considering the entire time axis (- ∞, + ∞), not the half-time one as usually considered in literature.

The gauge factor $\hbar\omega/k_{B}T<<1$ involved in the calculation can be studied for extending the use of the model from sub pico-level to macro-level.

a) Quantum behavior: the starting point is the effect of a frequency-dependent electric field of the form $\vec{E}=\vec{E}_{0}\,e^{i\omega t}$ considering the time-dependent perturbation theory, and handling the factor $e\vec{E}\cdot\vec{r}$ as perturbing potential ($\vec{r}$ = position vector of the particle) [38]. The matrix elements of the dipole moment of electron in the direction of the electric field, between the initial Φ_0 and the excited Φ_j states, are as follows:

$$e x_{j0}=\int\Phi_{j}^{*}\,e x\,\Phi_{0}\,dr \tag{40}$$

Defining the oscillator strength of the j-th transition as:

$$f_j = \frac{2m}{\hbar^2}\sum_j \hbar\omega_j \left|x_{0j}\right|^2 \tag{41}$$

and considering the relation between permittivity and conductivity of the system:

$$\varepsilon(\omega) = 1 + 4\pi i \frac{\sigma(\omega)}{\omega} = 1 + \frac{4\pi N e^2}{m}\sum_j \frac{f_j}{\omega_j^2 - \omega^2 + i\omega\Gamma_j} \tag{42}$$

the following relation is obtainable:

$$\frac{i\sigma(\omega)}{\omega} = \frac{1}{4\pi}\sum_i \frac{\omega_{p_i}^2}{(\omega_i^2 - \omega^2) - i\omega\Gamma_i} \tag{43}$$

with:

$${\omega_{p_i}}^2 = \frac{4\pi N e^2}{m} f_i \tag{44}$$

and:

- $\omega_i = (E_i - E_0)/\hbar$;
- E_0, E_i = energies of ground and excited states respectively;
- $\Gamma_i = 1/\tau_i$ = inverse of the decay time of every mode;
- N = density of carriers.

The weights f_i are the key factors including the quantum behavior. It holds: $\sum_i f_i = 1$.

b) Relativistic behavior: considering relativistic velocities of carriers inside a nanostructure, the starting point is the dynamics law:

$$\frac{d}{dt}(m_{part}\vec{v}) = \sum_i \vec{F}_i \tag{45}$$

About the forces acting on the generic carrier, it has been taken into consideration an outer passive elastic-type force of the form $F_{el} = Kx$, a passive friction-type force of the form $F_{fr} = \lambda\dot{x}$, with $\lambda = m_{part}/\tau$, and an outer oscillating electric field $E = eE_0 e^{-i\omega t}$ [39].

c) The quantum-relativistic version of the model incorporates both previous features. The general analytical calculation gives the following results:

(Q-R) Quantum-Relativistic case:

Q-R1) Case $\Delta_{iR_{Q-R}} > 0$

$$\left\langle \vec{v}(0)\cdot\vec{v}(t)\right\rangle = \left(\frac{k_B T}{m_0}\right)\left(\frac{1}{\gamma\rho}\right)\sum_i \Bigg(\left(f_i \exp\left(-\frac{t}{2\rho\tau_i}\right)\right)\left[\cos\left(-\frac{\alpha_{iR_{Q-R}}}{2\rho}\frac{t}{\tau_i}\right)-\frac{1}{\alpha_{iR_{Q-R}}}\sin\left(-\frac{\alpha_{iR_{Q-R}}}{2\rho}\frac{t}{\tau_i}\right)\right]\Bigg) \tag{46}$$

$$R^2(t)=2\left(\frac{k_B T}{m_0}\right)\sum_i \left[\left(\frac{f_i}{\omega_i^{\,2}}\right)\left(-\frac{1}{\alpha_{iR_{Q-R}}}\sin\left(\frac{\alpha_{iR_{Q-R}}}{2\rho}\frac{t}{\tau_i}\right)\exp\left(-\frac{t}{2\tau_i\rho}\right)-\cos\left(\frac{\alpha_{iR_{Q-R}}}{2\rho}\frac{t}{\tau_i}\right)\exp\left(-\frac{t}{2\tau_i\rho}\right)+1\right)\right], \tag{47}$$

$$D(t)=2\left(\frac{k_B T}{m_0}\right)\left(\frac{1}{\gamma}\right)\sum_i \left\{\left(\frac{f_i\tau_i}{\alpha_{iR_{Q-R}}}\right)\left[\exp\left(-\frac{1}{2\rho}\frac{t}{\tau_i}\right)\sin\left(\frac{\alpha_{iR_{Q-R}}}{2\rho}\frac{t}{\tau_i}\right)\right]\right\} \tag{48}$$

with:

$$\alpha_{iR_{Q-R}}=\sqrt{4\gamma\omega_i^2\tau_i^{\,2}-1}\ \in\Re^+ \quad \text{(positive real numbers)} \tag{49}$$

Q-R2) Case $\Delta_{iI_{Q-R}}<0$

$$\left\langle \vec{v}(0)\cdot\vec{v}(t)\right\rangle = \frac{1}{2}\left(\frac{k_B T}{m_0}\right)\left(\frac{1}{\gamma\rho}\right)\sum_i \Bigg(\left(\frac{f_i}{\alpha_{iI_{Q-R}}}\right)\left[\left(1+\alpha_{iI_{Q-R}}\right)\exp\left(-\frac{(1+\alpha_{iI_{Q-R}})}{2\rho}\frac{t}{\tau_i}\right)-\left(1-\alpha_{iI_{Q-R}}\right)\exp\left(-\frac{(1-\alpha_{iI_{Q-R}})}{2\rho}\frac{t}{\tau_i}\right)\right]\Bigg) \tag{50}$$

$$R^2(t)=4\left(\frac{k_B T}{m_0}\right)(\gamma)\sum_i \left\{\left(f_i\tau_i^{\,2}\right)\left[\frac{1}{\alpha_{iI_{Q-R}}\left(1+\alpha_{iI_{Q-R}}\right)}\exp\left(-\frac{(1+\alpha_{iI_{Q-R}})}{2\rho}\frac{t}{\tau_i}\right)-\frac{1}{\alpha_{iI_{Q-R}}\left(1-\alpha_{iI_{Q-R}}\right)}\exp\left(-\frac{(1-\alpha_{iI_{Q-R}})}{2\rho}\frac{t}{\tau_i}\right)+\frac{2}{\left(1-\alpha^2_{iI_{Q-R}}\right)}\right]\right\} \tag{51}$$

$$D(t)=\left(\frac{k_B T}{m_0}\right)\left(\frac{1}{\gamma}\right)\sum_i \left\{\left(\frac{f_i\tau_i}{\alpha_{iI_{Q-R}}}\right)\left[\exp\left(-\frac{(1-\alpha_{iI_{Q-R}})}{2\rho}\frac{t}{\tau_i}\right)-\exp\left(-\frac{(1+\alpha_{iI_{Q-R}})}{2\rho}\frac{t}{\tau_i}\right)\right]\right\} \tag{52}$$

with:

$$\alpha_{iI_{Q-R}}=\sqrt{1-4\gamma\omega_i^2\tau_i^{\,2}}\ \in(0,1)\subset\Re \tag{53}$$

It holds: $\alpha_{iI_{Q-R}}=\sqrt{\Delta_{iI_{Q-R}}}$, $\alpha_{iR_{Q-R}}=\sqrt{\Delta_{iR_{Q-R}}}$, $\gamma=1\big/\sqrt{1-\beta^2}$, $\beta=v/c$, $\rho=1+\beta^2\gamma^2=\gamma^2$ [40-42].

9. CONCLUSIONS

This work presents an overview of the analytical theoretical modeling concerning the transport (nano-)processes, considering the main formulations, with indications of the most used numerical approaches. Particular attention has been done to the Drude-Lorentz type models and to a recent extension formulated at quantum-relativistic level. This extension is mathematically highly elegant, being totally analytical, and fit very well with the previous models.

The new model, interpretable also as a plasmon model, is useful both to discover new features and to verify existing experimental data ("a priori" and "a posteriori" approach) as alternative to other generalizations of the Drude model. Among the principal findings, there is the reversal of the current in systems like nanoparticles and the time dependence of the transport parameter D, which describes the system dynamics for short and long time intervals, with increased mobilities at very short times followed by localization at longer times.

This particular behavior converges as a whole in the particular frequency dependence of the optical conductivity. It is one of the strengths of this model, i.e., its ability to accommodate this behavior and at the same time to include previous models, like the Smith model.

The obtained results allow the detailed study of transport dynamics, considering also quantum and relativistic effects, opening the way at phenomenological level to the detailed study of quantum phenomena and to the extreme fast carrier injection.

From a mathematical point of view, we have high refinement, considering its analytical formulation; it is an attractive novelty, which can be profitably object of experimental investigation through time-resolved techniques, like TRTS, PINEM, Graphene based Plasmonics [43-48].

Considering all parameters that can influence a system at a chemical, physical, and structural level (temperature T of the system, values of relaxation times τ_i and frequencies ω_i, carrier density N, effective mass m^*, variations of the chiral vector, quantum weights of each mode, velocity of carriers), and also the intrinsic parameters (values of $\alpha_{iR_{Q-R}}$ and $\alpha_{iI_{Q-R}}$), it is possible to perform a precise tuning of $\langle \vec{v}(t)\cdot\vec{v}(0)\rangle_T$, $R^2(t)$, and $D(t)$.

10. APPENDIX

In this Appendix, we present some of the various applications of the DS model in relation to currently most commonly materials considered in nanotechnology, such as zinc oxide (ZnO), titanium dioxide (TiO_2), gallium arsenide (GaAs), silicon (Si), carbon nanotubes (CNTs), and "last generation" materials, like Cadmium Telluride (CdTe), Cadmium Sulfide (CdS), Copper Indium Selenide (CIS), Copper Indium Gallium Selenide (CIGS).

1) TiO_2 nanostructure. Considered parameters: temperature $T = 300\ K$, effective mass $m^* = 6\ m_e$ (m_e = electron mass). The behavior of $\langle \vec{v}(t)\cdot\vec{v}(0)\rangle_T$ vs t/τ for two values of the parameter α_R ($\Delta > 0$) ($\alpha_{R1} = 10$; $\alpha_{R2} = 20$) (classical case). It is $\tau = 0.1\cdot10^{-13}\ s$. We note the classical damped oscillating behavior (Figure 1) [49].

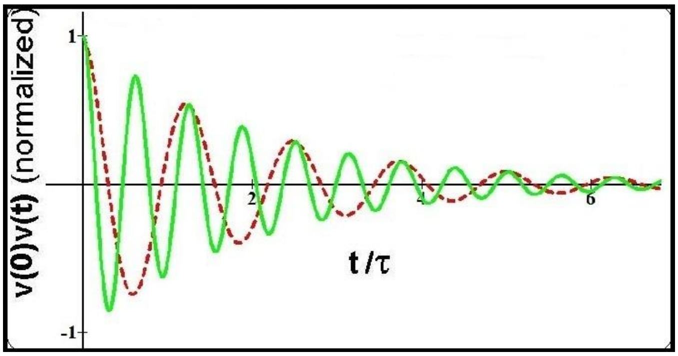

Figure 1. TiO_2 nanostructure (classical case) ($\Delta > 0$).

2) As the previous case, but considering α_I ($\Delta < 0$) ($\alpha_{I1} = 0.1$; $\alpha_{I2} = 0.5$; $\alpha_{I3} = 0.9$). Excluding the Drude case ($\omega_o = 0$), the velocities correlation function is a combination of exponentials. The results give a precise indication on response times of a system subjected to charge motion (Figure 2) [49].

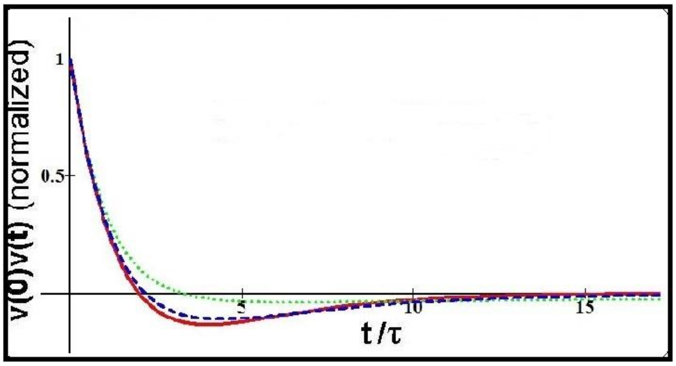

Figure 2. TiO_2 nanostructure (classical case) ($\Delta < 0$).

3) The velocities correlation function has been compared with the fit of experimental data using TiO_2; similar results are considering different materials. The result is predicted by the Smith model too, but with the DS model it appears without assumptions similar to the transport parameters cn of the Smith model (Figure 3) [49].

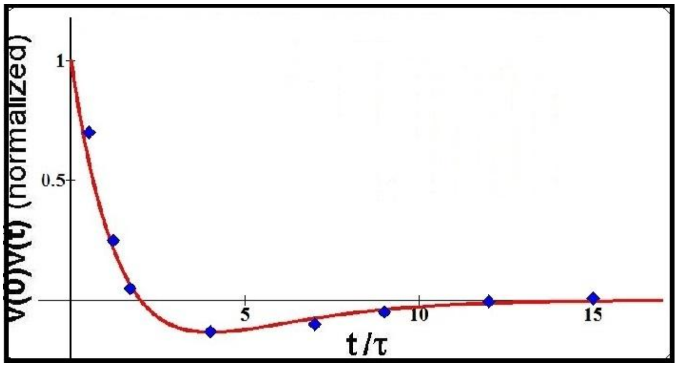

Figure 3. Dots represent experimental data, the curve derives by the DS model (classical case).

4) R^2 (x 10^{-14} cm^2) vs t/τ for some representative values of τ (of order of 10^{-13} s - 10^{-14} s), typical of doped Si ($T = 300\ K$) (Figure 4) [49].

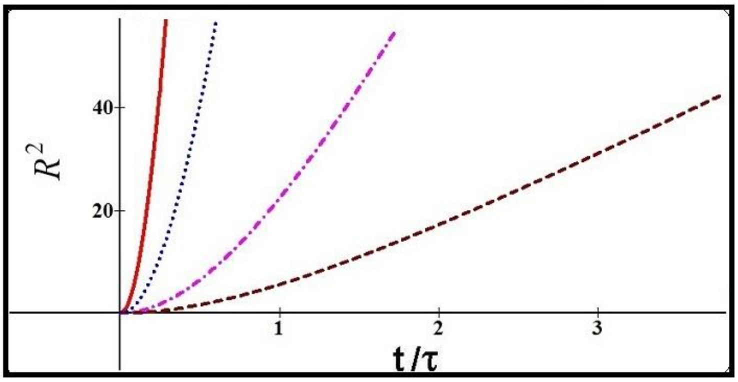

Figure 4. Doped Si (classical case).

5) R^2 (x 10^{-14} cm^2) vs t/τ for two values of τ ([illegible] dashed line; [illegible] solid line) for TiO_2 nanoparticle films ($m^* = 6\ m_e$, $T = 300\ K$), considering long times $x = t/\tau >> 1$. Curves reach a plateau value at sufficiently long times; the plateau of R^2 may become larger than the size of nanoparticles (Figure 5) [49].

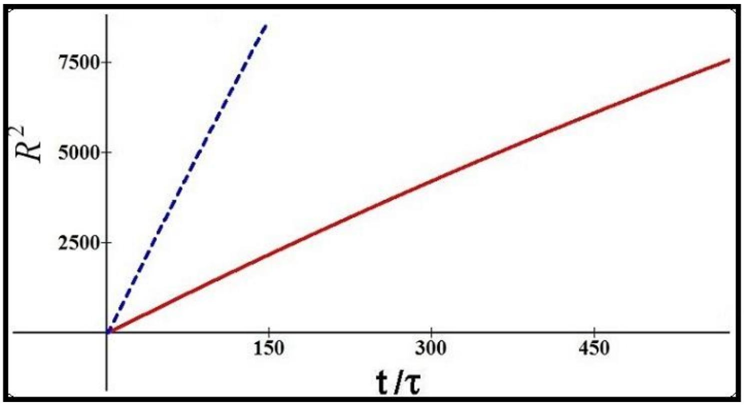

Figure 5. TiO2 nanoparticle film (classical case).

6) Diffusion coefficient D as a function of time considering a ZnO nanostructure, with [illegible] and for some values of the parameter α_1 (Figure 6) [49].

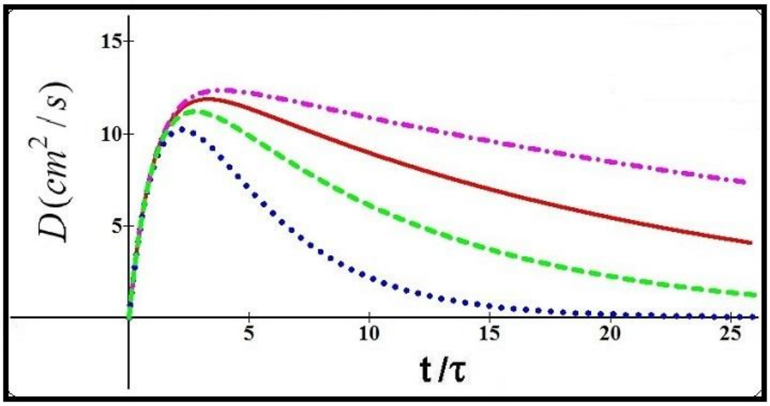

Figure 6. ZnO nanostructure (classical case).

7) Diffusion coefficient *D* for α_1 varying in the interval (0.1-1); dots represent experimental data of GaAs photo-conductivity with respective error bars (Figure 7) [49].

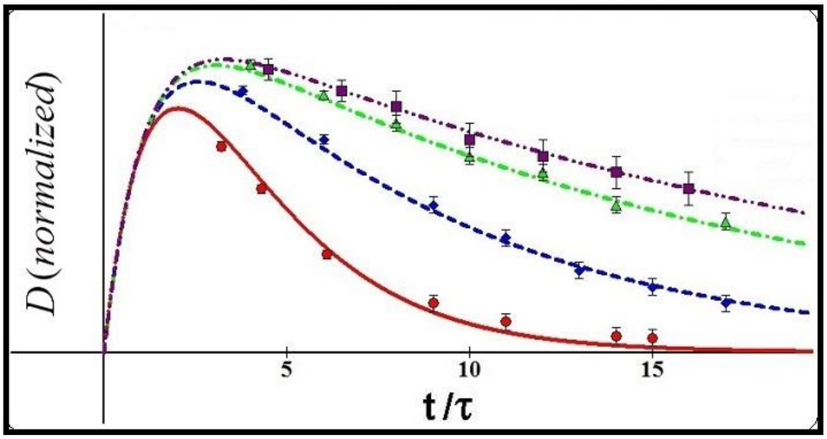

Figure 7. GaAs photo-conductivity (classical case).

8) $\langle \vec{v}(t)\cdot\vec{v}(0)\rangle_T$ vs *t* for CNTs in the quantum case, with data derived by literature, considering three weights with following parameters (Figure 8) [49]:

f_0 [illegible]

f_1 [illegible]

f_2 [illegible].

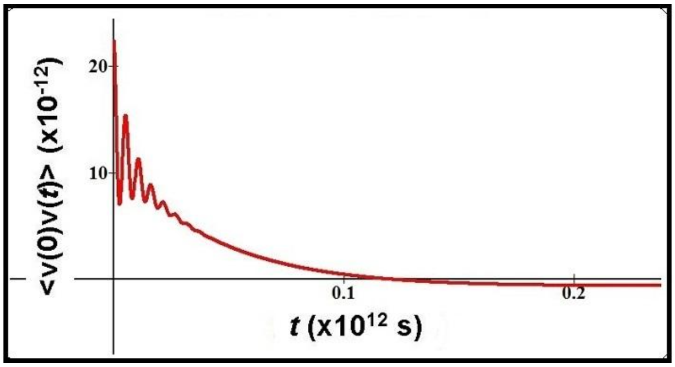

Figure 8. CNTs (quantum case).

9) Motion of electrons, at different velocities, inside a nanostructure of ZnO (relativistic case), for fixed value $\alpha_{R_{rel}}=5$; the velocities of carriers are $v=10^7\ cm/s$ (solid line), $v=10^{10}\ cm/s$ (dashed line) and $v=2\cdot 10^{10}\ cm/s$ (dots line); $\tau=0.84\cdot 10^{-13}\ s$ and $T=300\ K$ (Figure 9) [49].

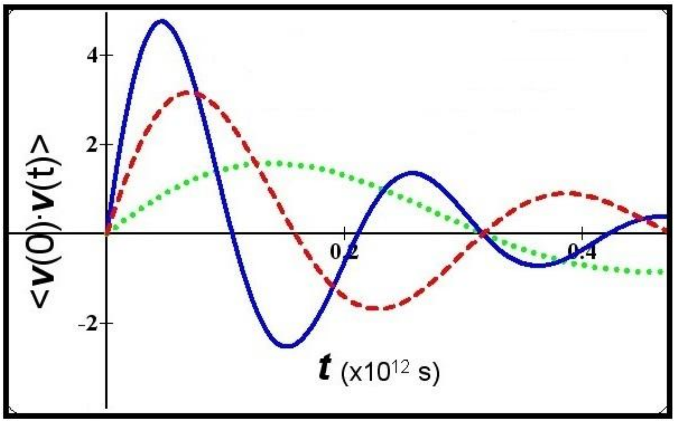

Figure 9. Nanostructure of ZnO (relativistic case).

10) Quantum-relativistic case: behavior of $\langle \vec{v}(t)\cdot\vec{v}(0)\rangle_T$ vs *t* for CNTs (Figure 10) [40].

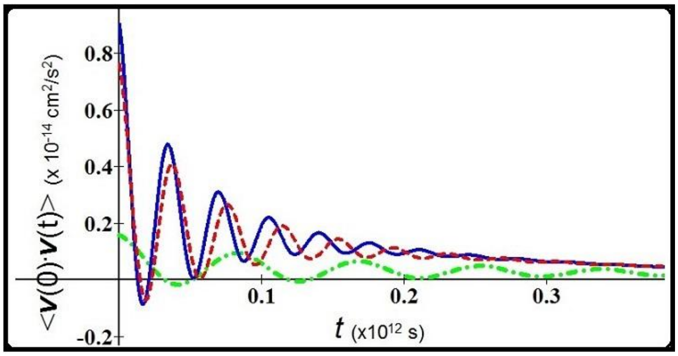

Figure 10. CNTs (quantum-relativistic case).

11) Quantum-relativistic case: behavior of R^2 vs t for ZnO (Figure 11) [41].

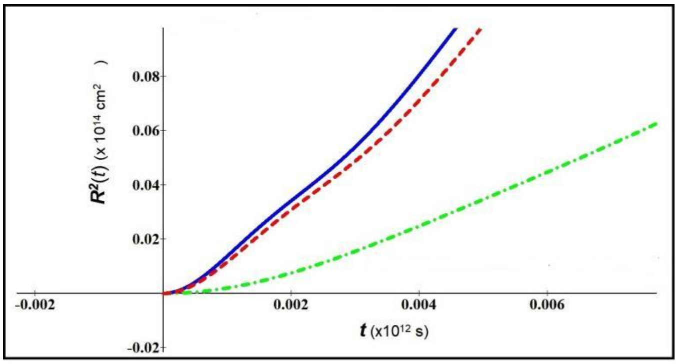

Figure 11. ZnO (quantum-relativistic case).

12) Quantum-relativistic case: behavior of D vs t for CNTs. (Figure 12) [42,50].

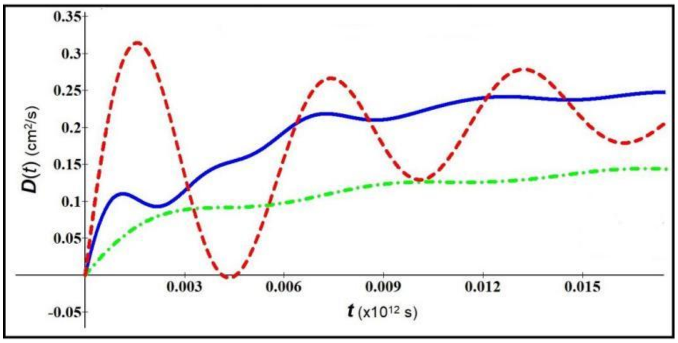

Figure 12. CNTs (quantum-relativistic case).

Author Contributions: Conceptualization, methodology, software, validation, formal analysis, investigation, resources, data curation, writing-original draft preparation, writing-review and editing, visualization, supervision, project administration, Paolo Di Sia.

Funding: This research received no external funding.

Data Availability Statement: Unavailable.

Acknowledgments: Unavailable.

Conflicts of Interest: The author declares no conflicts of interest.

Use of AI: AI tools and technologies have not been used in this article.

Biography

Paolo Di Sia (Adj. Prof., Dr., Dr., Dr.) is currently Adjunct Professor by the Universities of Padova and Verona (Italy), already Adj. Prof. by the Universities of Pavia and Bolzano-Bozen (Italy), Visiting Professor by the "National Center for Theoretical Sciences" (National Chiao Tung University, Hsinchu, Taiwan ROC), qualified as Associate Professor in Mathematics Didactics - Mathematics in Western Norway University of Applied Sciences, Norwegian University of Science and Technology (NTNU).

Universitetet i Agder, Nord Universitet, Universitetet i Stavanger, Oslo Metropolitan University (Norway), and Head of the "Primordial Dynamic Space" Research in Verona (Italy).

He got a Bachelor in Metaphysics, a Master in Theoretical Physics, and three PhDs (Mathematics, Theoretical Physics applied to Nanotechnology, Philosophy of Science).

His scientific interests span transdisciplinary physics, classical and quantum-relativistic nanophysics, nano-biotechnology, nano-neuroscience, (holistic) theories of everything, foundations of physics, history and philosophy of science, and science education.

He is author of hundreds of works to date (papers on national and international journals, book's chapters, books, inner academic works, works on scientific web-pages, popular papers), is reviewer of some academic books, editor of some international academic books, reviewer of many international journals.

He obtained several international awards, is member of many Scientific Societies, and International Advisory/Editorial Boards.

Personal web page: https://paolo-di-sia.weebly.com

References

[1] Di Sia P (2011). An Analytical Transport Model for Nanomaterials. *Journal of Computational and Theoretical Nanoscience* 8, 84-89. https://doi.org/10.1166/jctn.2011.1663.

[2] Hughes TJR (2000). *The Finite Element Method: Linear Static and Dynamic Finite Element Analysis*. Dover Publications, Mineola, NY.

[3] Bucalem ML, Bathe K-J (2011). *The Mechanics of Solids and Structures - Hierarchical Modeling and the Finite Element Solution*. Springer, Berlin, Heidelberg.

[4] Di Sia P (2014). Overview of Drude-Lorentz type models and their applications. *Nanoscale Systems: Mathematical Modeling, Theory and Applications* 3(1), 1-13. https://eudml.org/doc/267041.

[5] Cleland AN (2003). *Foundations of Nanomechanics: From Solid-State Theory to Device Applications*. Springer, Berlin, Heidelberg.

[6] Àlvarez FX, Cimmelli VA, Jou D, Sellitto A (2012). Mesoscopic description of boundary effects in nanoscale heat transport. *Nanoscale Systems: Mathematical Modeling, Theory and Applications* 1, 112-142. https://eudml.org/doc/266781.

[7] Panasenko G (2005). *Multi-scale Modelling for Structures and Composites*. Springer, Berlin, Heidelberg.

[8] Attinger S, Koumoutsakos PD (2004). *Multiscale Modelling And Simulation*. Springer, Berlin, Heidelberg.

[9] Binder K, Heermann DW (2010). *Monte Carlo Simulation in Statistical Physics: An Introduction*. Springer, Berlin, Heidelberg.

[10] Abdi A, Schulz D (2024). Application of the tight-binding method onto the Von Neumann equation. *Journal of Computational Electronics* 23, 707-717. https://doi.org/10.1007/s10825-024-02173-6.

[11] Jones RO (2015). Density functional theory: Its origins, rise to prominence, and future. *Reviews of Modern Physics* 87, 897. https://doi.org/10.1103/RevModPhys.87.897.

[12] Parr RG, Gadre SR, Bartolotti LJ (1979). Local density functional theory of atoms and molecules. *Proceedings of the National Academy of Sciences of the USA* 76(6), 2522-2526. https://doi.org/10.1073/pnas.76.6.2522.

[13] Engel E, Dreizler RM (2011). *Density Functional Theory. An Advanced Course*. Springer, Berlin, Heidelberg. https://doi.org/10.1007/978-3-642-14090-7.

[14] Car R, Parrinello M (1985). Unified Approach for Molecular Dynamics and Density-Functional Theory. *Physical Review Letters* 55(22), 2471. https://doi.org/10.1103/PhysRevLett.55.2471.

[15] Avriel M (2003). *Nonlinear Programming: Analysis and Methods*. Courier Dover Publications, Garden City, NY.

[16] Thijssen J (2007). *Computational Physics*. Cambridge University Press, Cambridge.

[17] Mizutani U (2001). *Introduction to the Electron Theory of Metals*. Cambridge University Press, Cambridge.

[18] Bland JAC, Bretislav H (2005). *Ultrathin Magnetic Structures I: An Introduction to the Electronic, Magnetic and Structural Properties*. Springer, Berlin, Heidelberg.

[19] Wandelt K (2012). *Surface and Interface Science*. John Wiley & Sons, Hoboken, NJ, vols 1-2.

[20] Wang J (2010). *Key Issues of Classical Molecular Dynamics Simulation*. Lambert Academic Publishing, Saarbrücken, Germany.

[21] Vinogradov SS, Smith PD, Vinogradova ED (2010). *Canonical Problems in Scattering and Potential Theory Part II: Acoustic and Electromagnetic Diffraction by Canonical Structures*. CRC Press, Boca Raton, FL.

[22] Fong CY, Shaughnessy M, Damewood L, Yang LH (2012). Theory, Experiment and Computation of Half Metals for Spintronics: Recent Progress in Si-based Materials. *Nanoscale Systems: Mathematical Modeling, Theory and Applications* 1, 1-22. https://eudml.org/doc/266869.

[23] Burkhardt CE, Leventhal JJ (2008). *Foundations of Quantum Physics*. Springer, Berlin, Heidelberg.

[24] Musa SM (2012). *Computational Finite Element Methods in Nanotechnology*. CRC Press, Boca Raton, FL.

[25] de Borst R, Ramm E (2011). *Multiscale Methods in Computational Mechanics: Progress and Accomplishments*. Springer, Berlin, Heidelberg.

[26] Mielke L, Belytschko T, Schatz GC (2007). Nanoscale Fracture Mechanics. *Annual Review of Physical Chemistry* 58, 185-209. doi: 10.1146/annurev.physchem.58.032806.104502.

[27] Gates TS, Odegard GM, Frankland SJV, Clancy TC (2005). Computational materials: Multi-scale modeling and simulation of nanostructured materials. *Composites Science and Technology* 65(15-16), 2416-2434. https://doi.org/10.1016/j.compscitech.2005.06.009.

[28] Shipway AN, Katz E, Willner I (2000). Nanoparticle arrays on surfaces for electronic, optical and sensoric applications. *ChemPhysChem* 1(1), 18-52. doi: 10.1002/1439-7641(20000804)1:1<18::AID-CPHC18>3.0.CO;2-L.

[29] Hutter E, Fendler JH (2004). Exploitation of Localized Surface Resonance. *Advanced Materials* 16(19), 1685-1706. https://doi.org/10.1002/adma.200400271.

[30] Gupta MC, Ungaro C, Foley IV JJ, Gray SK (2018). Optical nanostructures design, fabrication, and applications for solar/thermal energy conversion. *Solar Energy* 165, 100-114. https://doi.org/10.1016/j.solener.2018.01.010.

[31] Ranjan M (2013). Predicting plasmonic coupling with Mie–Gans theory in silver nanoparticle arrays. *Journal of Nanoparticle Research* 15, 1908. https://doi.org/10.1007/s11051-013-1908-7.

[32] Yurkin MA, Hoekstra AG (2022). The discrete dipole approximation: an overview and recent developments. arXiv:0704.0038v2 [physics.optics]. https://doi.org/10.48550/arXiv.0704.0038.

[33] Pan Y-L, Aptowicz K, Arnold J, Cheng S, Kalume A, Piedra P, Wang C, Santarpia J, Videen G (2022). Review of elastic light scattering from single aerosol particles and application in bioaerosol detection. *Journal of Quantitative Spectroscopy and Radiative Transfer* 279, 108067. https://doi.org/10.1016/j.jqsrt.2022.108067.

[34] Drude P (1900). Zur Elektronentheorie der metalle. *Annalen der Physik* 306(3), 566. https://doi.org/10.1002/andp.19003060312.

[35] Bethe HA, Sommerfeld A (1967). *Elektronentheorie der Metalle*. Springer, Berlin, Heidelberg.

[36] Choy TC (1999). *Effective Medium Theory: Principles and Applications*. Oxford University Press, Oxford.

[37] Smith NV (2001). Classical generalization of the Drude formula for the optical conductivity. *Physical Review B* 64, 155106. https://doi.org/10.1103/PhysRevB.64.155106.

[38] Di Sia P (2012). An Analytical Transport Model for Nanomaterials: The Quantum Version. *Journal of Computational and Theoretical Nanoscience* 9(1), 31-34. https://doi.org/10.1166/jctn.2012.1992.

[39] Di Sia P (2014). Relativistic nano-transport and artificial neural networks: details by a new analytical model. *International Journal of Artificial Intelligence and Mechatronics* (IJAIM) 3(3), 96-100. https://www.ijaim.org/vol-issues.html?view=publication&task=show&id=95.

[40] Di Sia P (2018). Quantum-Relativistic Velocities in Nano-Transport. *Applied Surface Science* 446, 187-190. https://doi.org/10.1016/j.apsusc.2018.01.273.

[41] Di Sia P (2023). Symmetry and the Nanoscale: Advances in Analytical Modeling in the Perspective of Holistic Unification. *Symmetry* 15(8), 1611. https://doi.org/10.3390/sym15081611.

[42] Di Sia P (2025). Beyond Drude-Lorentz-like Models: the Analytical Quantum-Relativistic Diffusion Function. *World Scientific News* 201, 15-25. https://worldscientificnews.com/beyond-drude-lorentz-like-models-the-analytical-quantum-relativistic-diffusion-function/.

[43] Baxter JB, Schmuttenmaer CA (2006). Conductivity of ZnO nanowires, nanoparticles, and thin films using time-resolved terahertz spectroscopy. *Journal of Physical Chemistry B* 110(50), 25229-25239. doi: 10.1021/jp064399a.

[44] Barwick B, Flannigan DJ, Zewail AH (2009). Photon-induced near-field electron microscopy. *Nature* 462, 902-906. doi: 10.1038 / nature08662.

[45] Park ST, Lin M, Zewail AH (2010). Photon-induced near-field electron microscopy (PINEM): theoretical and experimental. *New Journal of Physics* 12, 123028. doi: 10.1088/1367-2630/12/12/123028.

[46] Park ST, Zewail AH (2012). Relativistic Effects in Photon-Induced Near Field Electron Microscopy. *Journal of Physical Chemistry A* 116(46), 11128-11133. doi: 10.1021/jp304534n.

[47] Grigorenko AN, Polini M, Novoselov KS (2012). Graphene plasmonics. *Nature Photonics* 6, 749-758. doi:10.1038/nphoton.2012.262.

[48] Huang S, Song C, Zhang G, Yan H (2017). Graphene plasmonics: Physics and potential applications. *Nanophotonics-Berlin* 6(6), 1191-1204. doi: 10.1515/nanoph-2016-0126.

[49] Di Sia P (2019). *Mathematics and Physics for Nanotechnology - Technical Tools and Modelling*. Pan Stanford Publishing, Singapore. https://www.crcpress.com/Mathematics-and-Physics-for-Nanotechnology-Technical-Tools-and-Modelling/Sia/p/book/9789814800020.

[50] P. Di Sia P (2025). *On the Help of Mathematical-Analytical Modeling for Present and Future Advances in Current Engineering*. Preprints 2025, 2025082064.
https://doi.org/10.20944/preprints202508.2064.v1.